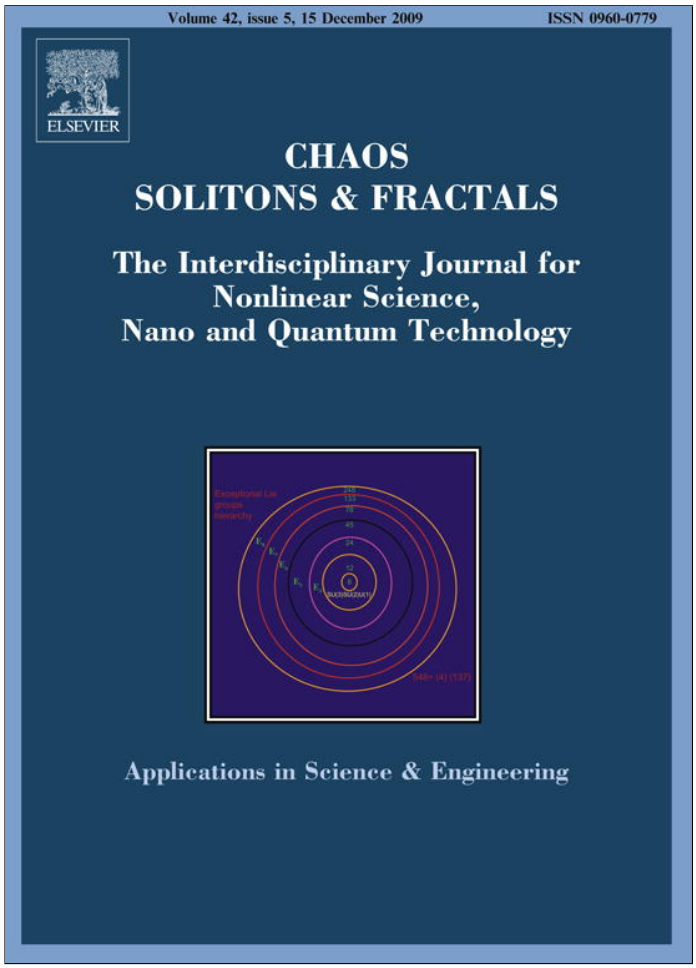

Chaos, Solitons and Fractals 42 (2009) 2875–2884

Contents lists available at ScienceDirect

Chaos, Solitons and Fractals

journal homepage: www.elsevier.com/locate/chaos

One-dimensional drug release from finite Menger sponges: In silico simulation

Rafael Villalobos [a,*], Armando Domínguez [b], Adriana Ganem [a], Ana Maria Vidales [c], Salomón Cordero [b]

[a] División de Estudios de Posgrado (Tecnología Farmacéutica), Facultad de Estudios Superiores Cuautitlán, Universidad Nacional Autónoma de México, Av. Primero de Mayo S/N, Cuautitlán Izcalli 54740, Estado de México, Mexico
[b] UAM-Iztapalapa, Depto. de Química, Av. San Rafael Atlixco 186, Col. Vicentina, 09340 Mexico City, Mexico
[c] Laboratorio de Ciencia de Superficies y Medios Porosos, Departamento de Física, CONICET, Universidad Nacional de San Luis, 5700 San Luis, Argentina

ARTICLE INFO

Article history:
Accepted 1 April 2009

ABSTRACT

The purpose of this work was to evaluate the consequences of the spatial distribution of components in pharmaceutical matrices type Menger sponge on the drug release kinetic from this kind of platforms by means of Monte Carlo computer simulation. First, six kinds of Menger sponges (porous fractal structures) with the same fractal dimension, $d_f = 2.727$, but with different random walk dimension, $d_w \in [2.149, 3.183]$, were constructed as models of drug release device. Later, Monte Carlo simulation was used to describe drug release from these structures as a diffusion-controlled process. The obtained results show that drug release from Menger sponges is characterized by an anomalous behavior: there are important effects of the microstructure anisotropy, and porous structures with the same fractal dimension but with different topology produce different release profiles. Moreover, the drug release kinetic from heteromorphic structures depends on the axis used to transport the material to the external medium. Finally, it was shown that the number of releasing sites on the matrix surface has a significant impact on drug release behavior and it can be described quantitatively by the Weibull function.

1. Introduction

The release of chemical entities from matrix systems is a widely used method in many industrial areas. In the pharmaceutical field the matrix supports are very useful for the development of controlled release pharmaceutical dosage forms [1]. This kind of dosage forms release the chemical entities in such a way that modulates the drug concentrations in the body allowing an optimum therapeutic effect with a minimum of adverse reactions [2]. It is because of this that the drug release profile from these platforms is fundamental for their better development. In the simplest case, a pharmaceutical matrix system includes two components: an inert material (excipient) and a water soluble material (drug). It has been shown both, experimentally [3] and through computer simulations [4], that the distribution of the components of the matrix system determines its transport properties, which in turn determine the drug release kinetics from the matrix platform. This binary system of a soluble drug and a plastic substance forming a matrix device becomes porous during the drug release [5]. Percolation models have been used to develop controlled release tablets. It has been shown that a percolation system has inherently associated a fractal structure close to its percolation threshold. Moreover, it has been demonstrated that the fractal dimension of the porous platform resulting from a fixed mixing ratio depends on the particle size of the soluble drug and the value of d_f was in the range 2.670–2.837. That is why, the Menger sponge, a fractal 3D structure with $d_f = 2.727$, has

* Corresponding author. Tel.: +52 5556232065.
E-mail address: yeccanv@yahoo.com (R. Villalobos).

0960-0779/$ - see front matter © 2009 Elsevier Ltd. All rights reserved.
doi:10.1016/j.chaos.2009.04.007

been used as a matrix model [6–11] and recently has been applied to the study of drug release [5,12]. Classical Menger sponge is a special class of three-dimensional fractals. It is created by sectioning a unit cube by slits of width 1/3. The central piece and each cube located at the center of the faces are removed. This process is repeated forever with the resulting cubes. This construction procedure repeated ad infinitum generates a self-similar Menger sponge. This structure shows a fractal space of dimension 2.727 and has a log-normal distribution with respect to the pore size presenting a total connectivity ($Q_c = 1$), i.e., there is not blind porosity, to any initial drug load [5].

In a previous work, we studied the release from the Menger sponges studied here using the total area of the device [12]. In such study it was possible to demonstrate that porous structures with same fractal dimension, $d_f = 2.727$, but with different internal structural characteristics showed different release behavior. However, by exposing all the surface of the device is more difficult to adjust the release behavior to a defined equation, so working with two opposite faces we reduce the release to a one-dimensional case and, on the other hand, releasing in one-dimensional form we can chose platforms with exactly the same specific surface and in consequence the influence of the internal morphology of the matrix platform can be evaluated specifically.

Despite the complexity of the drug release mechanism from porous matrices, three mathematical models are commonly used to describe the release profile: the square-root time law, the power law and the Weibull model. These models are mentioned next:

1.1. The square-root time law

This model [13] commonly describes the drug release from matrix systems, for a plane sheet system:

$$\frac{M_t}{M_\infty} = K_H t^{1/2} \tag{1}$$

where M_t is the amount of drug release from the matrix at a certain time t, M_∞ represents the maximum amount of drug released from the matrix and K_H a constant. This model is useful when the release is given from an homogeneous matrix, the mass transfer is one-directional and the fraction released is under 60%.

1.2. Power law

This equation is described as

$$\frac{M_t}{M_\infty} = Kt^n \tag{2}$$

where K is an experimentally determined parameter and n is a real number related to the structure of the drug releasing system. Ref. [14] used the value of n to characterize different release mechanisms, getting values for a block, of $n = 0.5$ for a Fickian diffusion and n values different from 0.5 for a mass transference that follows a non Fickian model. This equation is a generalization of the square-root time law and is useful to interpret the release behavior.

1.3. Weibull model

This model starts from a general empirical equation that was adapted to the dissolution/release process [15] and has recently been related to fractal kinetics [16]. This equation can be expressed as

$$\frac{M_t}{M_\infty} = 1 - \exp(-at^b) \tag{3}$$

In this equation the parameter a defines the time scale of the process, b represents the shape parameter. This parameter characterizes the shape of the curve, which can be exponential ($b = 1$), sigmoid or in S shape with a rising curve followed by an inflection point ($b > 1$), or parabolic with a higher initial slope that later gets consistent with the exponential ($b < 1$) [17]. The Weibull equation now has been deduced from kinetic concepts [16]. In that study it has been demonstrated that the parameter b is related to the internal structure of the medium, whereas the a parameter is related to the specific surface of the matrix [18]. In [16] to deduce the Weibull equation, they start with

$$\frac{dN}{dt} = -af(t)N \tag{4}$$

where a is a proportionality constant, fN denotes the number of particles that are able to reach an exit in a time interval dt, and the negative sign means that N decreases with time. If we assume the presence of interactions between the particles, this is an additional constraint implying that f should be a function of time. The reason is that as time elapses a large number of particles leave the structure, and the rest can move more freely. This has to be included somehow in the equation, and the way they propose to do this is through f. When $f(t)$ is equal to t^{-m} the Weibull equation can be reached. These researchers stated that there exist several different choices for the form of $f(t)$, and some of them might be better than the Weibull equation. However, the advantage of this choice is that it is general enough to allow us to describe release from devices of various

shapes, in the presence or absence of interactions, in Euclidean or fractal spaces, by adjusting the values of the parameters a and b.

The last equation has proved useful to describe the release profiles from cubic networks, both Euclidian and fractal [16,19], however, the fractals studied so far have been percolation fractals from a square lattice (2D). For this research drug release profiles are generated by means of computer simulation from different Menger sponges (three-dimensional deterministic fractal). These sponges present the same fractal dimension but different random walk fractal dimension. Finally, the results were analyzed using the three drug release models mentioned before and under concepts of fractal kinetics.

2. Methodology

For this study the matrix system is represented as a regular cubic network with L^3 sites. Within this network, the excipient is placed according to the Menger sponge. The Menger sponge is created by sectioning the unit cube by slits of width 1/3 as shown by the generator in Fig. 1. The central piece and each cube, of side length 3^{-1}, located at the center of the faces are removed in the first iteration resulting in a system of eight corner cubes being connected with twelve bridging cubes. In the second iteration seven cubes of side length 3^{-2} are removed from each of the remaining 20 cubes of the first iteration. This process, with the corresponding length scale, is repeated forever with the resulting cubes. The resulting body is known as the classical Menger sponge. In this work, the used network size was $L = 27$, which corresponds to a three-iteration of the Menger sponge. Six different Menger sponges were used for this research, all of them being of deterministic type. The basic structure (the position vectors (x,y,z) correspond to the axes shown in Fig. 1) that are taken out in each iteration are as follows: (2,2,1), (2,3,1), (1,3,2), (2,2,2), (3,2,2), (2,1,3), (1,3,3) for substrate *AMS*; (1,3,1), (2,3,1), (1,3,2), (1,2,2), (1,1,3), (1,3,3), (3,2,3) for substrate *BMS*; (2,2,1), (2,1,2), (1,2,2), (2,2,2), (3,2,2), (2,3,2), (2,2,3) for substrate *CMS*; (3,3,2), (3,1,3), (3,1,2), (2,3,3), (1,3,2), (1,3,1), (1,2,2) for substrate *DMS*; (2,2,1), (1,1,1), (2,1,2), (1,2,2), (3,2,2), (2,3,2), (2,2,3) for substrate *EMS*; (2,2,1), (2,1,1), (2,1,2), (1,2,2), (3,2,2), (2,3,2), (2,2,3) for substrate *FMS*. After that, the network was filled with drug in each of the seven cubes taken out from the corresponding iteration. The remaining spaces were assigned to sites used by the excipient. After three iterations the resulting solid fraction is 0.4064. In Fig. 2 the drug loaded Menger sponges after three iterations are shown. In this figure the faces of each sponge are labeled with the idea to quantify the number of leak sites and to show the spatial distribution of these sites on the surface of the device. On the other hand, for comparative purposes, we construct a percolated matrix system. The latter matrix system is represented as a regular cubic network with L^3 sites, where $L = 27$. This is, the pharmaceutical tablet is represented as a conglomerate of sites of the same size. Some sites of this network are taken by the drug and some others by the excipient. This network is filled randomly following a drug/excipient ratio of 0.5936/0.4064. Once formed, the networks were subjected to a release algorithm.

The release algorithm is simulated by a diffusive process of the drug within the matrix carcass which is generated by a random walk. It consists in the following: a site occupied by drug was randomly chosen; then, one of the six nearest neighboring sites is randomly chosen. If this chosen neighboring site is empty, the drug moves to this site, if the site is not empty, i.e., is occupied by drug or excipient, the drug particle stays in place. This sequence is repeated until the drug ends in a

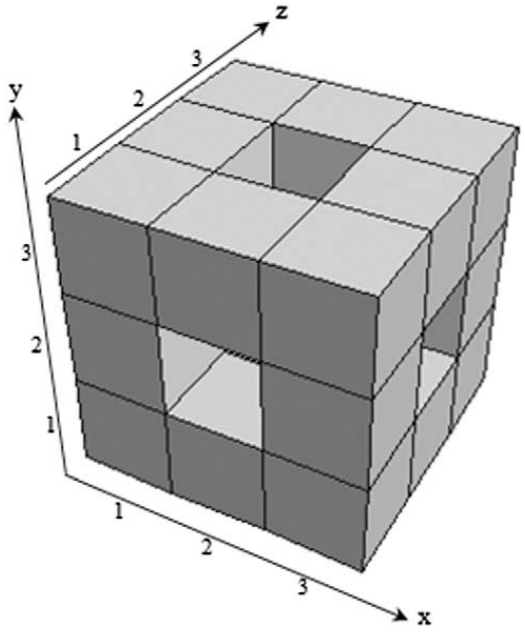

Fig. 1. Illustration of the classical Menger sponge generator and the axes of the vectors position.

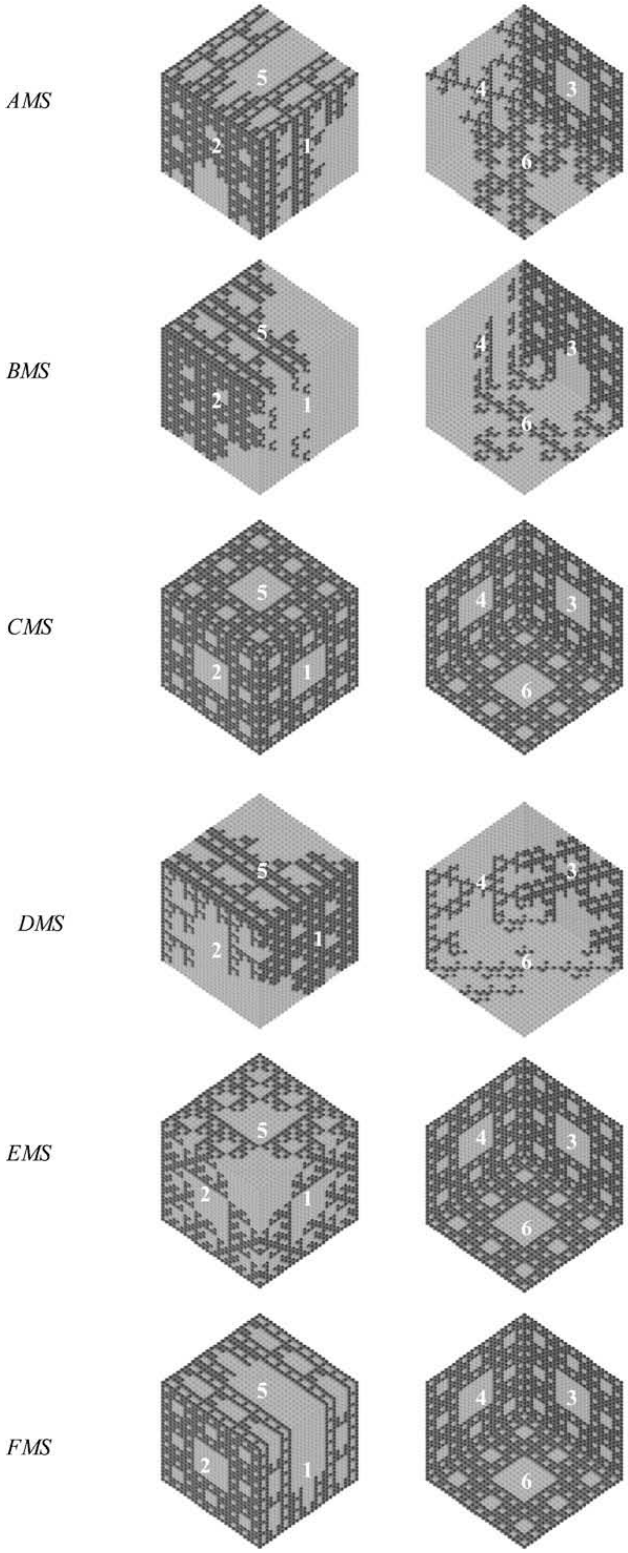

Fig. 2. Menger sponges. Network size $L = 27$, three iterations. Each face of the different structures is labeled by numbers. The sites in gray color represent drug particles, while the sites in black color represent the matrix carcass.

peripheral site, where it becomes part of the dissolution media. The previous algorithm described for the diffusion and later release is implemented randomly to all the network; this is, the N_t particles are randomly chosen, where N_t is the number of drug particles remaining in the matrix when the time is equal to t and a time step is performed. The previous algorithm is executed again and another time step is performed; this is a Monte Carlo Step (*MCS*), the unit of time. The time and average release are recorded. For this research only the release by two opposite faces (one-dimensional) was essayed.

3. Results and discussion

The formed structures are shown in Fig. 2. In this figure, each side of the different structures is labeled. The faces of the sponges show the spatial arrangement of the drug on the matrix surface as a consequence of the generator algorithm that was applied. On the other hand, the drug release profiles from these structures are shown in Fig. 3. In this figure it can be observed that the *CMS* and *EMS* sponges show the same release profile, independently from the pair of exposed faces; the *FMS* sponge shows the same release profile for two combinations of faces and is different for the remaining combination. Finally the *AMS*, *BMS*, and *DMS* sponges present a release that is dependent on the pair of faces exposed.

The behavior of the *CMS* and *EMS* sponges is explained as follows. In the case of the classical Menger sponge the initial structure introduced in the algorithm produces a macro structure that is totally symmetrical and isomorphic. To analyze more this point, in the structure of the first iteration we have 27 cubes placed in a cubic arrangement, from these 27 cubes, the one in the center is eliminated, after this first operation the resulting structure is totally symmetrical. Then from the remaining 26 cubes on each of the frontal sides, the central cube is eliminated. This operation also keeps the symmetry of the porous structure. In this way, the release profiles from the *CMS* sponge when two opposite sides were exposed, was independent from the pair of sides taken. For the case of the *EMS* sponge a total symmetry is found again for any pair of sides exposed. The only difference between this structure and the classical Menger structure is that the central cube, which is eliminated for a classical Menger sponge, is not eliminated for the *EMS* structure and in its place, a cube of side length $L = 9$ from the corner of the figure (from the original iteration) is eliminated, by allowing the release through two opposite sides the subcube (the one eliminated from the corner), it always contributes with only one exposed side, independently from the pair of opposite faces through which the release process takes place, this creates an isomorphic structure, only by exposing one pair of opposite faces, thus allowing the release profile to be independent from the pair of exposed faces (see Fig. 3).

When the release profile of the classical Menger sponge was compared to the one of the cubic structure, both with an initial drug load of 0.5936, some differences were found (see Fig. 3). For example, at the beginning of the release ($t < 500$ *MCS*), the fastest release comes from the cubic structure due to the fraction of surface area exposed

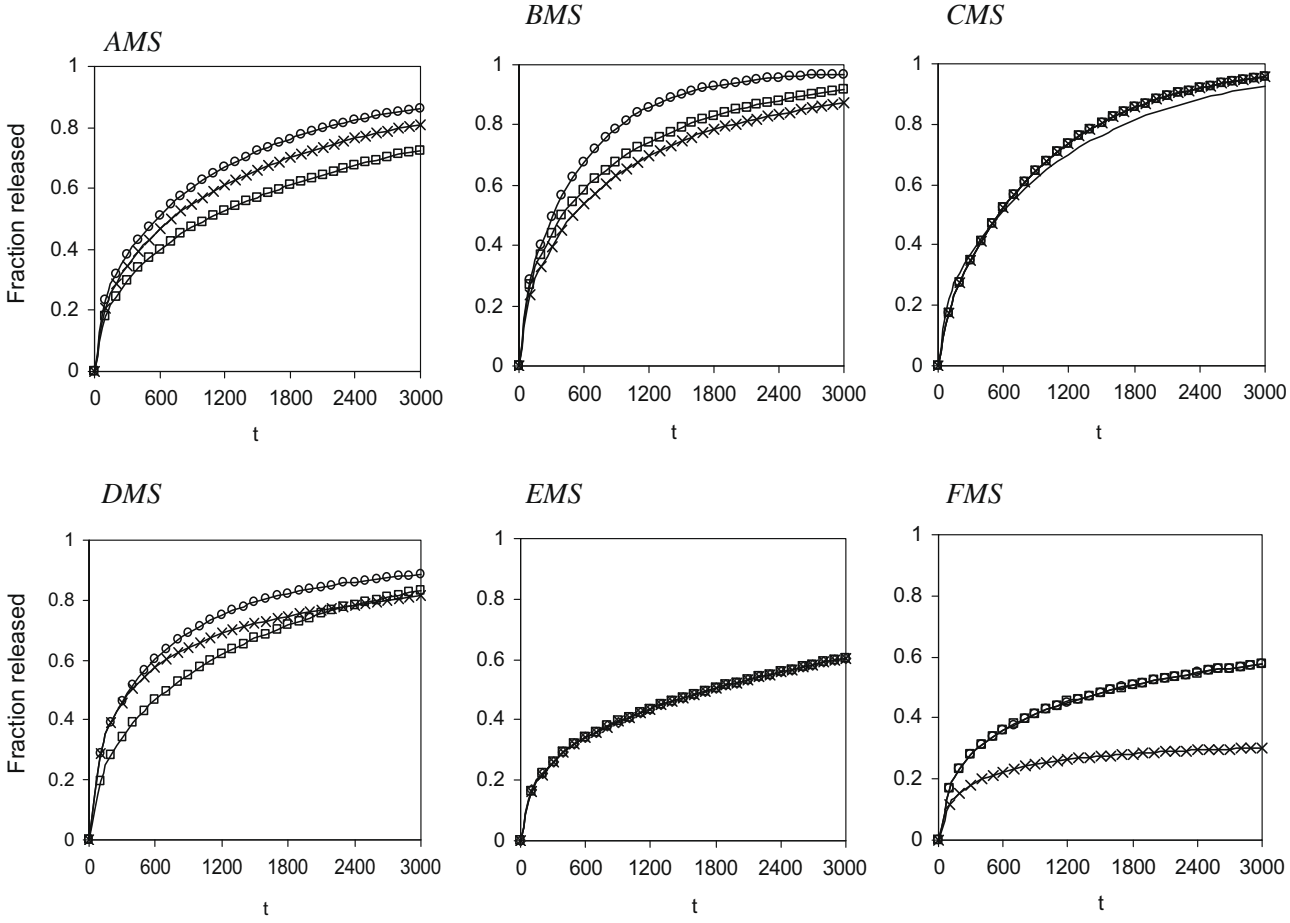

Fig. 3. Drug release from different Menger sponges. Network size $L = 27$, three iterations. The two opposite faces selected as release area were as follows: (□) face 1–3, (×) face 2–4, (○) face 5–6. For comparative purposes, in the figure corresponding to *CMS*, the release profile (continuous line) from a network created by de classical site percolation phenomenon through two opposite faces is also shown. For all the structures the initial drug load was 0.5936.

($N_{leak}/N_{total} = 0.0440$) being higher than that of the fractal structure of the classical Menger sponge ($N_{leak}/N_{total} = 0.0220$). After this difference in the release profiles, there is a point when both profiles are equal (approximately 500 *MCS*), and by the end of the process ($M_t/M_\infty > 0.5$) the fractal structure release is slightly faster than the matrix formed by a classical site percolation process because the fractal structure is related to a highly porous structure interconnected by great sizes pores.

A very interesting characteristic of the classical Menger sponge is its bicoherence; i.e., for the case in study each of the components, drug and excipient, forms an independent network that is totally interconnected in itself. The forming material of the insoluble carcass (excipient) forms an infinite cluster to any initial drug load, which produces a highly mechanical stability in this type of sponge. In the case of the drug, it forms a cluster through which it gets to any other particle of the soluble material, because of this, the initial drug load can be totally released, just like in the present simulations. This effect is not present in any of the other structures, see Table 1. This table shows the values for the amount released at an infinite time, when two opposite sides are exposed, for the different structures, the values for the relation N_{leak}/N_{total} are also shown, as well as the values of the fractal dimension of the random walk. These results show that the amount released of a drug after an infinite time was total for the *CMS* sponge; meanwhile the other structures showed an incomplete release after an infinite time, which is a function of the pair of exposed faces. This incomplete release shows that there are some drug particles that are not connected to the infinite drug cluster which is a result of the spatial distribution of the components within the matrix, and of the blockage of a great surface area; i.e., four faces of the matrix are not accessible to the external medium.

On the other hand, the *AMS*, *BMS*, *DMS* and *FMS* sponges generated a different release profile depending on the pair of exposed faces which demonstrates that these structures are heteromorphic, this is, their conformation is not the same in the different parts of the matrix, the tendency can be observed in Fig. 3. In the structure of the *AMS*, *BMS* and *DMS* Menger sponges any combination of opposite face pairs will always have a different external configuration (see Fig. 2), this is reflected on their release profiles which are different for the three combinations of each of the sponges. For the case of the *FMS* structure, two combinations of pairs of faces have the same external configuration, face 1–3 and face 5–6, and their release profiles were the same, which implies that not only the external configuration of the pairs of faces was the same but they also have the same internal morphology (statistically speaking). The other pair of faces, face 2–4, presented a different external structure, and this effect is reflected in a release profile that is different from those of the other two combinations of pairs of exposed faces. The external structure that showed this combination, face 2–4, was the same as that of a classical Menger sponge; however, the obtained release profiles are different from those obtained from a classical Menger sponge when exposing a pair of opposite faces. This indicates that in the release process not only the external conformation of the releasing surface is involved, but the internal morphology of the matrix, through which the diffusive process takes place, also plays a fundamental role.

In a general way it was found that the initial part of the release profile is determined by the amount of drug present on the surface (represented by the ratio N_{leak}/N_{total}), however this ratio continues affecting the phenomenon even at longer times, i.e., the amount of inner drug released from the matrix will depend on the number of exit sites (N_{leak}) in conjunction with the internal structural matrix properties, which are mentioned next. When the drug on the surface is released, the drug that is in the internal part of the structure starts to be moved, and from this point on, the properties associated to the interior of the matrix system modify the release profile of the drug. These properties are: the remaining amount of drug inside the matrix and the internal morphology of the porous system formed so far. To sustain these last two statements, we put together four profiles, from different sponges but with the same relation N_{leak}/N_{total} (0.0306), the structures are: *AMS* (1–3), *DMS* (1–3), *EMS*, and *FMS* (5–6). The release profiles from these structures are shown in Fig. 4. Here it is shown that the first part of the release is, in fact, determined by the relation N_{leak}/N_{total}, since below the 20% of the dose released, the release profiles are practically the same; however, after this point the differences are notable. In a previous work, the sponges *BSM* and

Table 1
Ratio of the number of leak sites and the total number of sites (N_{leak}/N_{total}), for different sponges exposing only two opposite faces, and the values for the amount of drug released at an infinite time (M_∞). Also is shown the fractal dimension of the random walk (d_w), after it traveled a distance of 13.5 (in lattice units).

Sponge	N_{leak}/N_{total}	M_∞	d_w
AMS (1–3)	0.0306	11007	2.712
AMS (2–4)	0.0370	10925	2.544
AMS (5–6)	0.0392	10955	2.668
BMS (1–3)	0.0448	11446	2.242
BMS (2–4)	0.0417	11436	2.216
BMS (5–6)	0.0456	11414	2.433
CMS	0.0220	11683	2.149
DMS (1–3)	0.0306	11236	2.566
DMS (2–4)	0.0521	11042	2.536
DMS (5–6)	0.0502	10777	2.582
EMS	0.0306	10108	3.161
FMS (1–3)	0.0306	9406	3.163
FMS (2–4)	0.0220	3718	3.079
FMS (5–6)	0.0306	9406	3.183

The relative error of d_w and M_∞ are bounded by 0.008 and 22, respectively.

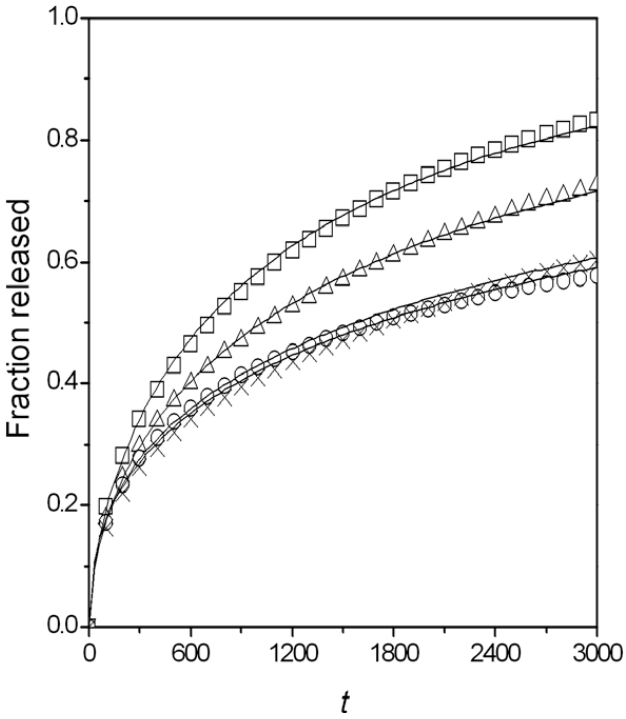

Fig. 4. Drug release from different Menger sponges with the same N_{leak}/N_{total} ratio (0.0306). Network size $L = 27$, three iterations. Two opposite faces were taken as the release area. Symbols represent the Monte Carlo simulation data, while solid lines are the corresponding fitting by Weibull model. (△) *AMS* (1–3), (□) *DMS* (1–3), (×) *EMS* (5–6), (○) *FMS* (5–6). For all the structures the initial drug load was 0.5936.

DMS exposing their total surface showed a similar behaviour [12]. It can be observed that there is a close relation between the number of particles available for release and the corresponding profile; for example, the Menger sponge *DMS* (1–3) presents the highest release profile and it also has the highest number of particles available for release which in turn is associated to higher concentration gradient. But the difference in the number of particles released at a time equal to infinite, M_∞, is not enough to explain the differences found in the release profiles. For example, the difference between the structures *AMS* (1–3) and *DMS* (1–3) is of 229 released particles at a time equal to infinite, and their corresponding release profiles move apart after releasing more than 20% of the dose. On the other hand, the difference of released amounts between the *EMS* and *FMS* structures at a time equal to infinite is of 700 particles and their release profiles are very similar, which implies that the internal morphology of the porous medium is actively participating in the shape of the release profile. This effect can be evaluated by means of a fractal dimension of the random walk, which indicates how easy it is for a particle to move through the porous medium. In the present case, structures with the same number of exit sites, *EMS* and *FMS* (5–6), had a d_w of 3.161 and 3.183, respectively, which are associated with the slowest release profiles. The *AMS* (1–3) structure showed a d_w of 2.712, and it was associated with a faster release than the two previous structures. Finally, *DMS* (1–3) had a d_w of 2.566 and presented the fastest release profile of the three previous cases. It is important to note that in a previous work it was determined the d_w of the latter sponges allowing the movement through the entire surface of the device [12]. In all cases this d_w was lower than that determined for the one-dimensional case. This phenomenon is due to the restriction of movement through four faces of the device makes the drug diffusion in this medium more difficult. This observation is important because d_w affects the parameters of the drug release kinetics. Then, it will be necessary to determine the d_w value in the one-dimensional or in the three-dimensional case to apply it to the mathematical model, respectively.

Since, in the present work we studied the one-dimensional drug release case, the square root of the time and the power law can give a straightforward idea of the release behaviour. The release profiles as a function of the square root of the time showed a linear behavior below 60% of the dose released. The latter was confirmed by a regression analysis (Table 2), where the determination coefficient (r^2) was found to be above 0.98 for almost all the sponges, except for a couple of combinations of the sponge *FMS*, *FMS* (1–3) and *FMS* (5–6), that showed an r^2 of about 0.96. Once again it is important to emphasize that the previous model, despite adjusting well until 60% of the release, does not describe properly the release process above this amount. Besides, while reviewing the data of the linear regression of the logarithm of the fraction of drug released versus the logarithm of the time (Table 3) it was found that this model fits the process well until 60% of release. The found exponents related to the time for the different Menger sponges correspond to an anomalous transport, associated in turn with the fractal structure of these sponges [20].

When the release data were treated with the Weibull model a good adjustment was found ($r^2 > 0.98$) taking into account values up to 90% of the dose released (see Table 4). When the constants obtained from the Weibull equation for isomorphic structures were compared, the classical Menger sponge showed a higher b than that of the *EMS* structure. While the constant

Table 2
Linear regression of the fraction released versus square root of the time, for different Menger sponges of $L = 27$, delivery occurs through two opposite faces. We use the initial 60% of the release data. K_H, in units of $1/MCS$, represents the slope in the relationship M_t/N_0 versus $t^{1/2}$.

Structure	r^2	K_H
AMS (1–3)	0.9919	0.01361
AMS (2–4)	0.9939	0.01704
AMS (5–6)	0.9948	0.01928
BMS (1–3)	0.9948	0.02305
BMS (2–4)	0.9968	0.02108
BMS (5–6)	0.9995	0.02848
CMS	0.9981	0.02323
DMS (1–3)	0.9959	0.01766
DMS (2–4)	0.9829	0.02141
DMS (5–6)	0.9927	0.02371
EMS	0.9888	0.00969
FMS (1–3)	0.9639	0.00882
FMS (2–4)	0.9867	0.03125
FMS (5–6)	0.9644	0.00882

r^2 determination coefficient, the relative error of K_H is bounded by 0.00062.

Table 3
Linear regression of $\log(M_t/N_0)$ versus $\log MCS$, for different Menger sponges of $L = 27$. Delivery occurs through two opposite faces and we use the initial 60% of the release data.

Structure	r^2	Exponent (n)
AMS (1–3)	0.99474	0.4415
AMS (2–4)	0.99238	0.4628
AMS (5–6)	0.99535	0.4607
BMS (1–3)	0.99497	0.4718
BMS (2–4)	0.99378	0.4855
BMS (5–6)	0.99819	0.5215
CMS	0.99889	0.6183
DMS (1–3)	0.99476	0.4848
DMS (2–4)	0.98786	0.4271
DMS (5–6)	0.99403	0.4561
EMS	0.99392	0.3883
FMS (1–3)	0.98107	0.3632
FMS (2–4)	0.98649	0.4695
FMS (5–6)	0.98107	0.3632

r^2 determination coefficient, the relative error of n is bounded by 0.0094.

Table 4
Fitting of Weibull equation to M_t/N_0, for different Menger sponges of $L = 27$. Delivery occurs through two opposite faces and we use the initial 90% of the release data.

Structure	r^2	a	b
AMS (1–3)	0.9993	0.01499	0.5534
AMS (2–4)	0.9991	0.01546	0.5816
AMS (5–6)	0.9984	0.01597	0.5999
BMS (1–3)	0.9990	0.01791	0.6125
BMS (2–4)	0.9995	0.01641	0.6042
BMS (5–6)	0.9959	0.01315	0.7009
CMS	0.9962	0.00484	0.7942
DMS (1–3)	0.9987	0.01246	0.6161
DMS (2–4)	0.9932	0.04055	0.4703
DMS (5–6)	0.9987	0.02614	0.5570
EMS	0.9817	0.02332	0.4608
FMS (1–3)	0.9953	0.02405	0.4516
FMS (2–4)	0.9988	0.03523	0.5530
FMS (5–6)	0.9955	0.02422	0.4506

r^2 determination coefficient. The relative error of a and b are bounded by 0.00095 and 0.0037, respectively.

a for the *EMS* structure had a higher value, this constant must be associated with higher release rate (at the beginning of the process) with respect to the one shown by the classical Menger sponge. In the case of the *AMS* Menger sponge, the three release profiles found for the three combinations of pairs of faces never intersected each other and the values of a and b were

in direct relation with the N_{leak}/N_{total} ratio of the corresponding combinations, i.e., the release rate follows the order: *AMS*(5–6) > *AMS*(2–4) > *AMS*(1–3), the N_{leak}/N_{total} values follow the order *AMS*(5–6) > *AMS*(2–4) > *AMS*(1–3), and the *a* and *b* constant values follow the order *AMS*(5–6) > *AMS*(2–4) > *AMS*(1–3). In the case of the *BMS* Menger sponge, constant *b* also showed a direct relation with the N_{leak}/N_{total} ratio, while it was not the case for constant *a*. In the case of the *DMS* sponge, the faces 5–6 and 2–4 showed a very similar release profile until a released fraction of about 0.5 and then they separated, when these profiles were adjusted to the Weibull equation, the constants are inverted, i.e., a high *b* value is combined with a low *a* value and vice versa. The case of the *FMS* Menger sponge the effect was similar.

Papadopoulou et al. have done an excellent work about the meaning of *b* value obtained from both, experimentally and with Monte Carlo computer simulations, release studies [21]. They made an analysis of the *b* value and the release mechanism. They found *b* values in the range 0.69–0.75 associated to drug release by diffusion in a normal Euclidian space, and *b* values in the range 0.35–0.69 related to drug release by diffusion in fractal or disordered substrate. In our study, only two combination shown *b* values higher than 0.69, the resting shown *b* values less than 0.69. The *b* values obtained in this study less than 0.69 are related with diffusion in fractal disordered spaces and is in concordance with the analysis made in [21]. The *b* value equal to 0.7942 obtained for *CMS* sponge can be explained as follows: the Menger sponge generator of side length $L = 3$ is connected to pores of side length $L = 3$, and as consequences of the generator these pores are connected to void channels of side length $L = 9$, generating in this way a highly easy release, it like from an homogeneous space (see Fig. 3 for *CMS* structure), the latter statement is corroborated by its $d_w = 2.149$, which is close to $d_w = 2$ that is found in an Euclidean space. In the case of *BMS* (5–6) the disorder is now presented and the *b* value is lower than in the *CMS* structure.

When the released profiles with the same N_{leak}/N_{total} ratio were analyzed, it was observed that the higher release profile is inherently associated with a higher *b* constant, e.g. confront the *DMS* Menger sponge face 1–3 ($b = 0.6161$) versus *AMS* Menger sponge face 1–3 ($b = 0.5534$). On the other hand, both profiles found below the profile that corresponds to the *AMS* Menger sponge, also showed lower *b* values; however, for a released fraction up to about 0.4 the release profile from the *EMS* structure is below that of the *FMS* despite having a lower *b* constant. Since the *a* constant is higher for *FMS* than for *EMS*, this combination leads to an intersection of the profiles. In a general way, even if the N_{leak}/N_{total} value impacts that of the *a* and *b* constants, the value of M_∞ must also participates as well as the internal morphology of the porous system. This last point, however, requires further research in order to determine in a more precise way the contribution of the previous parameters on the *a* and *b* constant values of the Weibull equation.

4. Conclusions

Computer simulations are useful tools in the study of drug release from matrix platforms, specially because they can describe the profile through the whole process. Menger sponges with exactly the same fractal dimension but with different topology show different drug release behaviors, being the specific surface area and the matrix internal structure two parameters that strongly affect the release profile. The random walk dimension can be used to quantitatively describe the internal structure of porous systems. Using this concept of dimension, in this study, it was demonstrated that the transport properties depend on the axis which the release is going on. This result will be useful to analyse the release from solids made by compaction specially when some preferential arrangement is present due to non equal radial and axial forces applied during the compression. On an other hand, the Weibull equation is a useful model to describe the release profiles generated from both fractal and Euclidian structures, and can be properly applied to the one-dimensional case. It was found that the specific surface of the device is defined by Weibull's *a* value while the transport mechanism is defined by Weibull's *b* value. However, future efforts are necessary to relate the values of *a* and *b* in the Weibull equation in such a way that their experimental determination gives a straightforward idea of the internal structure of the platform and vice versa.

Acknowledgements

This work was economically supported by CONACyT. Furthermore this work was supported by CONACyT (Mexico) – CONICET (Argentina) through project "Catálisis, Fisicoquímica de Superficies e Interfases Gas – Sólido" (2007). Thanks are also due to PIFI 3.1 (SEP-Mexico) project UAM-I-CA-31: "Fisicoquímica de Superficies".

References

[1] Takada K, Yoshikawa H. Oral drug delivery, traditional. In: Mathiowitz E, editor. Encyclopedia of controlled drug delivery. United States of America: Wiley; 1999. p. 728–42.
[2] Groves MJ. In: Mathiowitz E, editor. Encyclopedia of controlled drug delivery. USA: Wiley; 1999. p. 743.
[3] Leuenberger H, Bonny JD, Kolb M. Percolation effects in matrix-type controlled drug-release system. Int J Pharm 1995;115:217–24.
[4] Villalobos GR, Cordero S, Vidales AM, Dominguez OA. In silico study on the effects of matrix structure in controlled drug release. Physica A 2006;367:305–18.
[5] Usteri M, Bonny JD, Leuenberger H. Fractal dimension of porous solid dosage forms. Pharm Acta Helv 1990;65:55–61.
[6] Adler PM. Transports in fractal porous media. J Hydrol 1996;187:195–213.
[7] Karalis V, Claret L, Iliadis A, Macheras P. Fractal volume of drug distribution: it scales proportionally to body mass. Pharm Res 2001;18(7):1056–60.
[8] Kozak JJ. Random walks on the Menger sponge. Chem Phys Lett 1997;275:199–202.
[9] Leuenberger RL, Bonny JD. Percolation theory, fractal geometry and dosage form design. Pharm Acta Helv 1989;64:34–9.
[10] Leuenberger RL, Bonny JD. Application of percolation theory and fractal geometry to tablet compaction. Drug Dev Ind Pharm 1992;18:723–66.

[11] Pfeifer P, Avnir D. Chemistry in noninteger dimensions between two and three. I. Fractal theory of heterogeneous surfaces. J Chem Phys 1983;79(7):3558–65.
[12] Villalobos R, Vidales AM, Cordero S, Quintanar D, Domínguez A. Monte Carlo simulation of diffusion-limited drug release from finite fractal matrices. J Sol–Gel Sci Technol 2006;37:195–9.
[13] Higuchi T. Mechanism of sustained-action medication. Theoretical analysis of rate released of solid drugs dispersed in solid matrices. J Pharm Sci 1963;52:1145–8.
[14] Peppas N. Analysis of Fickian and non-Fickian drug release from polymers. Pharm Acta Helv 1985;60(4):110–1.
[15] Langenbucher F. Linearization of dissolution rate curves by the Weibull distribution. J Pharm Pharmacol 1972;24:979–81.
[16] Kosmidis K, Argyrakis P, Macheras P. Fractal kinetics in drug release from finite fractal matrices. J Chem Phys 2003;119(12):6373–7.
[17] Costa P, Sousa JM. Modeling and comparison of dissolution profiles. Eur J Pharm Sci 2001;13:123–33.
[18] Kosmidis K, Argyrakis P, Macheras P. A reappraisal of drug release laws using Monte Carlo simulations: the prevalence of the Weibull function. Pharm Res 2003;20(7):988–95.
[19] Bunde A, Havlin S, Nossal R, Stanley H, Weiss G. On controlled diffusion-limited drug release from a leaky matrix. J Chem Phys 1985;83(11):5909–13.
[20] Tarafdar S, Franz A, Schulzky K, Hoffmann K. Modelling porous structures by repeated Sierpinski carpets. Physica A 2001;292:1–8.
[21] Papadopoulou V, Kosmidis K, Vlachou M, Macheras P. On the use of the Weibull function for the discernment of drug release mechanisms. Int J Pharm 2006;309:44–50.